J. Chem. Sci. (2020)132:124
https://doi.org/10.1007/s12039-020-01828-8

REGULAR ARTICLE

Influence of sugars in preparing improved FeAl catalyst for carbon dioxide hydrogenation

WENSHENG NING*, BEI LI, HUI DAI, SHIYE HU, XIAZHEN YANG, BIAO WANG and BO ZHANG

College of Chemical Engineering, Zhejiang University of Technology, Hangzhou 310032, China
E-mail: wenshning@sohu.com; ningwensheng@zjut.edu.cn

MS received 16 November 2019; revised 26 June 2020; accepted 9 July 2020

Abstract. The influences of sugars (sucrose, fructose and glucose) on the performance of FeAl catalysts were investigated for CO_2 hydrogenation. FeAl catalysts were prepared with two steps. At first, the catalyst precursors were obtained by co-precipitation. During this step, three methods were used to add sucrose into the precursors. Then, promoter K and Cu were impregnated into the precursors. The improved CO_2 conversion and C_{5+} hydrocarbon selectivity by sucrose addition were attributed to the formation of γ-Fe_2O_3 phase in the catalyst precursor, which was different from the popular opinion that sucrose acted as a chelating agent. With the inspiration from sucrose hydrolysis effect, FeAl oxide, mainly in γ-Fe_2O_3 phase was prepared by adding fructose and glucose (the products of sucrose hydrolysis) into the newly centrifuged precipitate. The formation of γ-Fe_2O_3 phase was explained based on the results of XRD and XPS. The best catalyst possessed CO_2 conversion of 30.3% and C_5 + selectivity of 52.2% under the reaction conditions of H_2-:CO_2 = 3:1, 6.0 L/(h·g-cat), 1.6 MPa and 235 °C.

Keywords. Sucrose hydrolysis; CO_2 hydrogenation; γ-Fe_2O_3 phase.

1. Introduction

After carbon dioxide (CO_2) is recognized as one of the main factors inducing the global temperature increase and climate change, many measures have been put into practice to control its concentration in the atmosphere.[1,2] These measures can be classified into two groups, one is to avoid CO_2 formation and the other is to prevent CO_2 emission into the atmosphere. The first measure is to replace the traditional carbon-based fuels (coal, crude oil) with nuclear energy, solar energy, and wind energy, which do not produce CO_2 from their consumption. The second measure is to capture and store CO_2 (CCS) following the combustion of traditional carbon-based fuels. During the practice, some shortcomings are found in the two measures. For example, solar energy and wind energy intrinsically fluctuate with day/night cycles, or seasonal alternation.[3] CCS would potentially damage the ecosystem by environmental acidification. Therefore, an efficient and stable CO_2-declining method is evolved from the two measures, that is to store the intermittent solar and wind energy into combustible chemicals through CO_2 catalytic hydrogenation.[3–8]

Iron-based catalysts are good at synthesizing hydrocarbon molecules larger than methane from CO_2 hydrogenation.[9–11] Aiming to improve the performance of iron-based catalysts, the effects of the promoter,[4,9,11–14] supporter,[9,15] preparation method[2,9,14–17] and reducing agent[18] have been studied very much. The catalyst in γ-Fe_2O_3 phase is much active than that in α-Fe_2O_3 phase for the reaction.[16,19]

We have found that γ-Fe_2O_3 phase was formed in FeAl oxide only after the FeAl precipitate was washed by anhydrous ethanol, but there was obvious α-Fe_2O_3 phase coexisted in it.[19] Here, an easy method which can increase the purity of γ-Fe_2O_3 phase in FeAl oxide is reported. It is based on the reduction effect of fructose and glucose on Fe^{3+} ion.

*For correspondence

Electronic supplementary material: The online version of this article (https://doi.org/10.1007/s12039-020-01828-8) contains supplementary material, which is available to authorized users.

Published online: 11 September 2020

2. Experimental

2.1 *Catalyst preparation*

All the used metal salts are in analytical grade and purchased from Sinopharm Chemical Reagent Co., Ltd. Analytical pure Sucrose is from Guangdong Guanghua Sci-Tech Co., Ltd. D-Fructose and D-(+)-Glucose are from Aladdin Industrial Corporation with the purity of 99% and ≥ 99.5%, respectively.

Two solutions were prepared with distilled water at room temperature. One contained $(NH_4)_2CO_3$ in the content of 0.30 g/mL. Another was composed of 0.271 g/mL $Fe(NO_3)_3{\cdot}9H_2O$ and 0.0079 g/mL $Al(NO_3)_3{\cdot}9H_2O$. The two solutions were pumped simultaneously into a precipitated flask of 50 °C under vigorous stirring and pH = 7.0 ± 0.5. The precipitate and mother liquid were kept in the flask at 50 °C for 30 min, and then at room temperature for 60 min. Subsequently, the precipitate was separated from the liquid by centrifugation at 4000 RPM (Revolutions Per Minute) and 5 min. The precipitate was further washed by distilled water and centrifuged at 4000 RPM and 10 min for two times. After the precipitate was dried at 120 °C overnight and calcined at 350 °C for 6 h in stagnant air, it was pressed under 20 MPa for 2 min and cracked with agate mortar into particles of 150–300 μm, which was used as catalyst precursor and named as P-C. Sucrose (S) was added into the mixed $Fe(NO_3)_3$ and $Al(NO_3)_3$ solution (A), or $(NH_4)_2CO_3$ solution (B), or the final newly centrifuged precipitate (C), respectively. Correspondingly, the three precursors were remarked as P-*x*S-A, P-*x*S-B and P-*x*S-C. The *x* in the above names was the mass ratio of sucrose to Fe_2O_3 in percentage. In the case of fructose (F) and glucose (G) were used, the precursor was named in a similar style. For example, if fructose and glucose were added into the final newly centrifuged precipitate and blended homogeneously, the obtained precursor was recorded as P-*y*F*z*G-C. The *y* and *z* in the above names were the mass ratios of fructose and glucose to Fe_2O_3 in percentage, respectively. If *y* or *z* equals to zero, the F or G would be omitted from the sample name.

Promoter K and Cu were impregnated onto the precursors with the mass ratio of K/Fe_2O_3 = 1% and Cu/Fe_2O_3 = 4%, respectively. The promoted catalyst was titled with the corresponding precursor's name by deleting the initial "P-".

2.2 *Characterization*

The instruments and methods for the characterizations, such as texture structure, crystal structure (XRD) and temperature-programmed reduction (H_2-TPR) of the catalysts were given in previous work.[14] For the measurement of CO_2 temperature-programmed desorption (CO_2-TPD), 0.1 g sample was filled into the U-type quartz tube and pretreated by 50 mL/min CO at 300 °C for 2 h. Then, the sample was flushed with 30 mL/min Ar at 300 °C for 1 h and cooled to 100 °C. Subsequently, the reduced sample was contacted with 30 mL/min CO_2 at 100 °C for 1.5 h. After the sample was flushed by Ar (30 mL/min) for 0.5 h, it was heated to 850 °C at the rate of 10 °C/min in 30 mL/min Ar. The desorbed gas was analyzed by the mass spectrometer of Omnistar GSD301.

Sucrose hydrolysis was observed by WXG-4 Polarimeter (Shanghai INESA Physico-Optical Instrument Co., Ltd). The light source was the D-line of Na lamp (589 nm). The length of the sample tube was 10 cm, and the environmental temperature was 30 °C.

XPS analysis was done by K-Alpha + (Thermo Fisher Ltd.) using Al Kα radiation (1486.6 eV). The energy step size was 0.1 eV, and the peak positions were calibrated with the binding energy of C 1*s* (284.8 eV).

2.3 *Activity test and product analysis*

A detailed program to test the catalyst activity is shared in Supplementary Information.

3. Results and Discussion

3.1 *Influence of the methods to add sucrose*

Sucrose was applied to catalyst preparation in three methods. The mass ratio of sucrose to Fe_2O_3 was 50–200% for series A and B, and 10–40% for series C. According to Figure S1 (Supplementary Information), the catalysts prepared with the same method to add sucrose show similar reactivity regardless of the added amount. Based on Figure S1, the least amount of sucrose was chosen for the three preparation methods, respectively.

Table 1 lists the reactive performance of catalyst C, 50S-A, 50S-B and 10S-C. The data of catalyst 50S-B and 10S-C are similar to catalyst C, but 50S-A is different from them. 50S-A presents the highest CO_2 conversion, olefin/paraffin ratio in C_2-C_4 and C_{5+} hydrocarbons selectivity. The same correlation between olefin/paraffin ratio and long-chain hydrocarbons selectivity has been found for CO_2 hydrogenation[13,14] and CO hydrogenation.[20,21]

The four catalysts were analyzed by XRD, N_2 adsorption at low temperature and H_2-TPR. There is no apparent difference among the XRD patterns of the four catalysts (Figure S2, Supplementary Information), but catalyst 50S-A has the smallest surface area (Table S1, Supplementary Information). Figure 1a contrasts the reducibility of the precursors and catalysts. Two peaks are found for the four precursors. The first one in the range of 260–400 °C is from the reduction of Fe_2O_3 to Fe_3O_4, and the second in

Table 1. Reactive performance of catalysts with different methods to add sugars.

Sample	CO_2 conversion (%)	Selectivity (C mol%)				
		CO	CH_4	C_2–C_4 olefin	C_2–C_4 paraffin	C_5 + hydrocarbon
C	21.7	13.2	14.4	21.9	9.5	41.0
50S-A	25.5	10.8	11.1	19.1	6.8	52.2
50S-B	22.1	13.3	13.0	20.7	8.1	44.9
10S-C	22.5	12.2	13.9	19.9	9.8	44.2
26.3F26.3G-A	22.1	12.9	14.9	20.4	10.7	41.1
26.3F26.3G-B	25.2	11.4	13.2	18.2	9.0	48.2
26.3F26.3G-C	30.3	8.6	12.7	16.2	10.3	52.2

Reaction condition: H_2:CO_2:N_2 = 69:23:8, 6.0 L/(h·g-cat), 1.6 MPa, 235 °C.

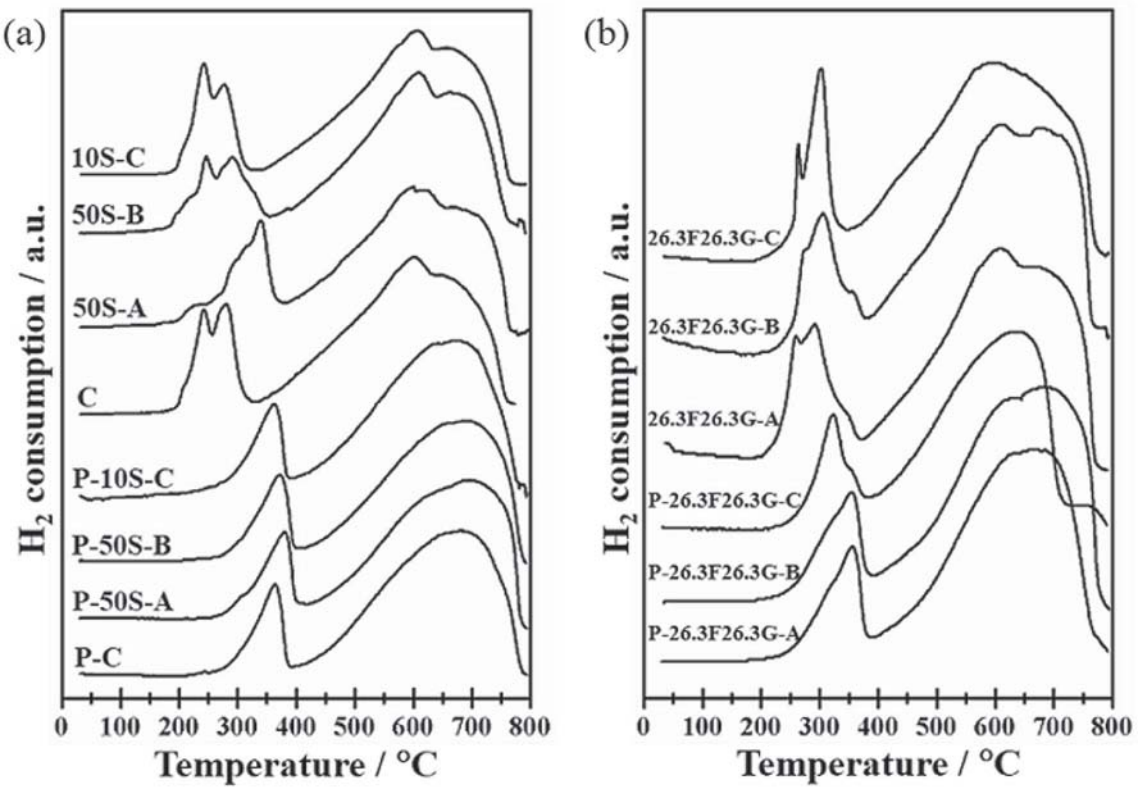

Figure 1. H_2-TPR of the precursors and catalysts. (a) Influence of sucrose addition. (b) Influence of fructose and glucose.

420–790 °C is the reduction of Fe_3O_4 to Fe. The iron oxide interacted with aluminium oxide was reduced in the second range,[22] too. The reduction temperature of P-50S-A is the highest among the four precursors for the reduction process of Fe_2O_3 to Fe_3O_4. After the precursors were impregnated with K and Cu, the reduction peaks shifted to low temperature by the help of Cu.[20,23] There are four peaks for catalyst C, 50S-B and 10S-C. The peak in 200–260 °C is from the reduction of CuO to Cu, and 260–350 °C is the reduction of Fe_2O_3 to Fe_3O_4. The promotion of Cu on the reduction makes the smooth peak above 420 °C of the precursors separated into two peaks. The one in 360–640 °C is from the reduction of Fe_3O_4 to Fe. Above 640 °C may be the reduction of iron oxide interacted with aluminium oxide.[22] 50S-A displays a wide peak below 380 °C, composed of the reduction of CuO to Cu and Fe_2O_3 to Fe_3O_4. According to the calculation based on Figure S2 (Supplementary Information), both CuO and Fe_2O_3 exist in a bigger size in 50S-A than the others. Big particles of CuO and Fe_2O_3 would weaken the contact between them, which

prevented the promoting effect of Cu on the reduction of Fe_2O_3.[20,23] As a result, the peak temperature is shifted to high.

In general, small surface area and low reducibility would lead to the less active site on the catalyst. Therefore, the reason why 50S-A is more active (Table 1) is worthy to be explored.

3.2 *Sucrose hydrolysis*

It is well known that sucrose can be hydrolyzed into fructose and glucose in acid solution,[24] which is depicted as Function (1). The pH value of $Fe(NO_3)_3$ solution is as low as 0.84, so that sucrose could be hydrolyzed in the process to prepare P-50S-A, because it was added into an acid solution.

$$C_{12}H_{22}O_{11}(\text{Sucrose}) + H_2O = C_6H_{12}O_6(\text{Fructose}) + C_6H_{12}O_6(\text{Glucose}) \quad (1)$$

Figure 2 is the optical rotation of $Fe(NO_3)_3$ and $Al(NO_3)_3$ solutions added with sucrose, and $(NH_4)_2CO_3$ solution with sucrose, respectively. Sucrose and glucose are right-handed chemicals with a specific rotation of $\langle\alpha\rangle_D^{20} = 66.37°$ and $\langle\alpha\rangle_D^{20} = 52.7°$, while fructose is left-handed with $\langle\alpha\rangle_D^{20} = -92°$. As a result, the observed angle would decrease if sucrose hydrolysis happened. The declined angle with time for $Fe(NO_3)_3$ and $Al(NO_3)_3$ solution discloses the occurrence of sucrose hydrolysis, which was the scene for P-50S-A. The unchanged angle of $(NH_4)_2CO_3$ solution confirms that sucrose is stable in alkaline solution.

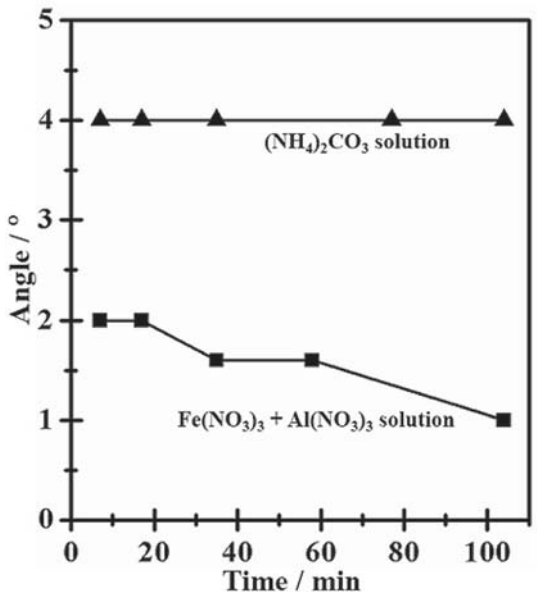

Figure 2. Optical rotation of the solutions with sucrose addition.

Because the precipitation reaction of $Fe(NO_3)_3$ and $Al(NO_3)_3$ by $(NH_4)_2CO_3$ was controlled at pH = 7.0 ± 0.5, sucrose hydrolysis was inhibited during the precipitation for P-50S-B. For P-10S-C, sucrose hydrolysis could not happen as the result that the sucrose was mixed with neutral precipitate.

The results in Figure 2 confirm that the sucrose hydrolysis happened in the mixed solution of $Fe(NO_3)_3$ and $Al(NO_3)_3$, but the derived catalyst 50S-A is similar to catalyst C given their crystal structure (Figure S2, Supplementary Information). The possible reason is that the degree of sucrose hydrolysis was too weak to change the bulk structure. Therefore, the solution of $Fe(NO_3)_3$ and $Al(NO_3)_3$ containing sucrose was heated to 50 °C and 60 °C, respectively. High temperature can enhance sucrose hydrolysis. The obtained catalyst precursors were analyzed by XRD and shown in Figure S4 (Supplementary Information). γ-Fe_2O_3 phase appears in P-50S-A-50 °C and P-50S-A-60 °C. It is acceptable to assign γ-Fe_2O_3 formation to the hydrolysates, fructose and glucose.

Sucrose has been used to prepare nano-powders,[25,26] and supported cobalt-based catalysts.[27–29] Its role is thought as a chelating agent for metal ions after it was oxidized to saccaric acid in the presence of nitric acid,[25–27] which results in a product with fine particles and high surface area. According to the surface area in Table S1 (Supplementary Information) and the crystal size calculated from Figure S2 (Supplementary Information), the chelating effect from sucrose only worked for 10S-C. Therefore, we think that the added sucrose should not be regarded only as chelating agent in this work. Depending on the added method, sucrose could be a reducing agent after it was hydrolyzed. This assumption will be discussed with XPS analysis in '3.3.3 XPS of catalysts'.

3.3 *Influence of fructose and glucose on catalyst*

3.3a *Catalytic performance*: As discussed in the above, the high performance of 50S-A is hypothetically related to sucrose hydrolysis, or the hydrolysates of fructose and glucose. In order to clarify the promoting mechanism, some catalysts were prepared with fructose and glucose. Their reactive performance is given in Table 1, too.

It can be concluded that fructose and glucose are better than sucrose to increase catalyst activity in the case adding fructose and glucose into $(NH_4)_2CO_3$ solution or the precipitate. In contrast, adding fructose and glucose into $Fe(NO_3)_3$ and $Al(NO_3)_3$ solution (Catalyst 26.3F26.3G-A) brought the lowest CO_2

conversion. The reactive performance of 26.3F26.3G-A is close to catalyst C and poorer than 50S-A. It is possible if fructose and glucose were dehydrated into sucrose via reverse-hydrolysis. The similar reactive performances of 50S-B and 10S-C to C have suggested that the sucrose existed in the precipitates is almost inert to influence the catalytic performance.

The reactive performance of 26.3F26.3G-C with time on stream is shown in Figure S5 (Supplementary Information). It quickly reached to the stable state. Although 26.3F26.3G-C was evaluated under lower temperature and higher gas hourly space velocity (GHSV), its performance was comparable or superior to other state of art catalysts[2,5,14,15,17,30,31] which are compared in Table S2 (Supplementary Information).

3.3b *XRD of precipitates before and after calcination*: Figure 3a compares the XRD results of dried precipitates of P-C with P-26.3F26.3G-C. Strong peaks appeared in P-C are respectively assigned to α-Fe_2O_3 (PDF: 33-0664) and FeO(OH) (PDF: 81-0462). These peaks are weakened into two wide envelopes after fructose and glucose were added. The formation and growth of crystals were inhibited by the added sugar during the drying.

After the calcination (Figure 3b), only α-Fe_2O_3 is detected in P-C. An evident change is happened in the precursors added with fructose and glucose. Besides the α-Fe_2O_3 peaks, strong γ-Fe_2O_3 (PDF: 39-1346) peaks can be seen in P-26.3F26.3G-A, P-26.3F26.3G-B and P-26.3F26.3G-C. The results in Figure 3b disclose that the addition of fructose and glucose is the factor to form γ-Fe_2O_3 phase in the precursors, which has been a hypothesis based on Figure S4 (Supplementary Information).

The method to add fructose and glucose determines the strength of γ-Fe_2O_3 peaks. The added sugar was basically remained in dried P-26.3F26.3G-C, but much sugar was lost in dried P-26.3F26.3G-A and P-26.3F26.3G-B. More sugar would bring heavier inhibition to the formation of thermodynamically preferential α-Fe_2O_3. P-26.3F26.3G-C is mainly constructed by γ-Fe_2O_3 phase. To use solely fructose or glucose can form γ-Fe_2O_3 phase, too (Figure S6, Supplementary Information).

Figure S7 (Supplementary Information) presents the XRD patterns of 26.3F26.3G-A, 26.3F26.3G-B and 26.3F26.3G-C. The operations of promoter impregnation and re-heating treatment did not weaken γ-Fe_2O_3 phase in the catalysts. 26.3F26.3G-C has the strongest γ-Fe_2O_3 phase and the weakest α-Fe_2O_3

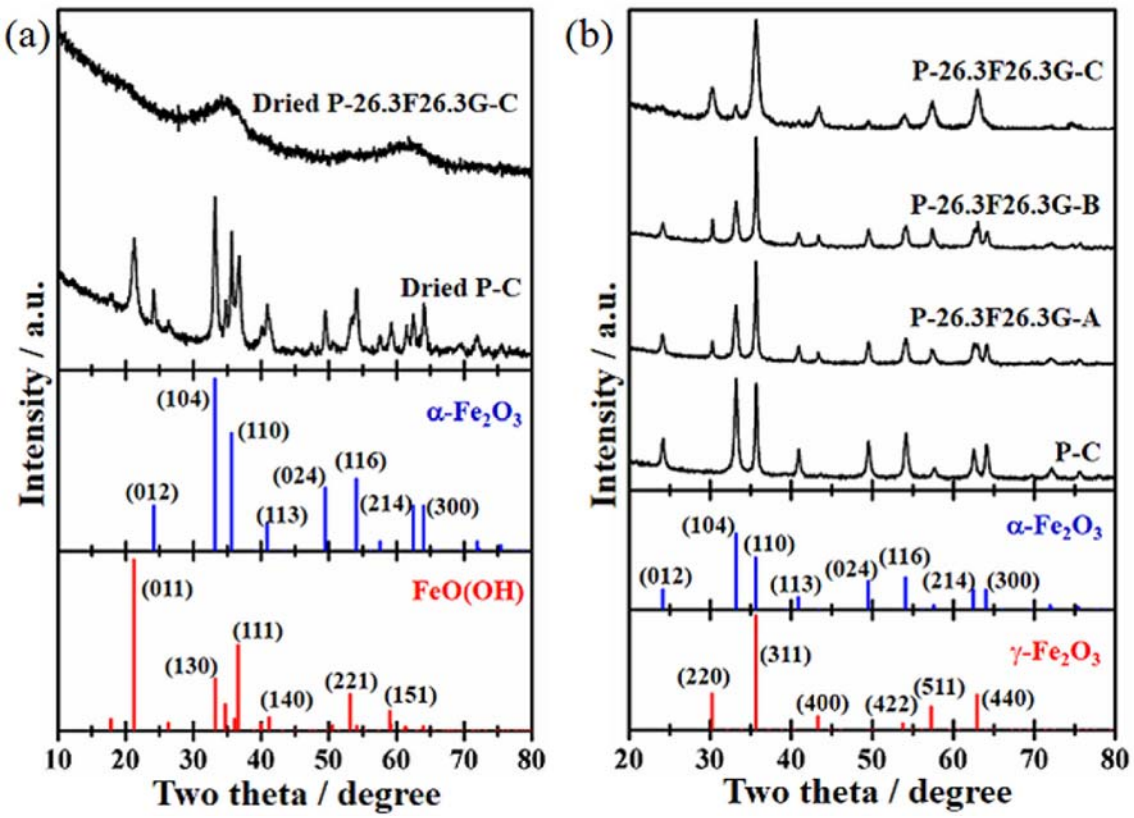

Figure 3. XRD patterns of precipitates before and after calcination. (a) Dried precipitates. (b) Calcined precipitates.

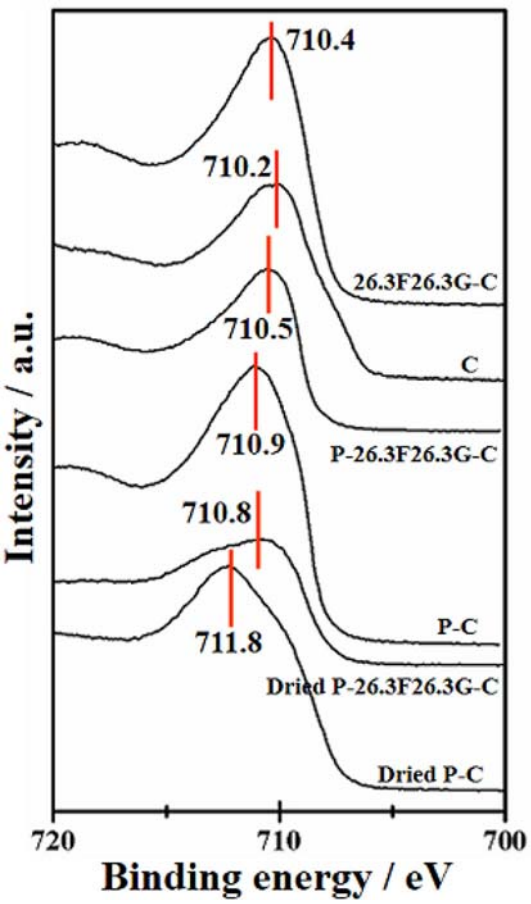

Figure 4. Fe $2p_{3/2}$ spectra influenced by added fructose and glucose.

phase. As shown in Table 1, 26.3F26.3G-C is the most active one. It has been reported that the iron-based catalyst in γ-Fe_2O_3 phases was more active than that in α-Fe_2O_3 phase for CO_2 hydrogenation.[16,19]

3.3c *XPS of catalysts*: The influence of fructose and glucose addition on catalysts' surface property were investigated by XPS. The samples were taken from the three stages of catalyst preparation, i.e., dried precipitate, calcined precipitate (precursor) and promoted catalyst.

Figure 4 is the binding energy (BE) of Fe $2p_{3/2}$ peaks. For the samples only dried at 120 °C, the BE of dried P-C is higher than dried P-26.3F26.3G-C. The BE of Fe^{2+} ion is lower than Fe^{3+} ion.[32] Furthermore, the asymmetric extension to higher BE supports the assignment of iron ion in dried P-26.3F26.3G-C to Fe^{2+} state.[33] On the contrary, the iron ion in dried P-C is in Fe^{3+} state. The only difference between the preparation methods of dried P-C and P-26.3F26.3G-C is whether fructose and glucose were added into the final newly centrifuged precipitate. With the addition of fructose and glucose, which are well known reducing agent, iron ion was reduced from Fe^{3+} to Fe^{2+}.

After calcination, the Fe $2p_{3/2}$ BE is down-shifted, but the value of P-C is still higher than P-26.3F26.3G-C. Figure 3b has disclosed that P-C is in α-Fe_2O_3 phase, and P-26.3F26.3G-C is mainly in γ-Fe_2O_3 phase. So, both the iron ion in P-C and P-26.3F26.3G-C can be assigned as Fe^{3+}. It has been discussed based on Figure S4 (Supplementary Information) that the formation of γ-Fe_2O_3 phase is related to the reducing ability of fructose and glucose. The mechanism is probably that Fe^{3+} ion from $Fe(NO_3)_3$ is reduced into Fe^{2+} by fructose and glucose in the precipitation and drying. Although the Fe^{2+} ion is re-oxidized into Fe^{3+} during the calcination, metastable γ-Fe_2O_3 phase is formed with the help of low calcining temperature (350 °C). We have found that only α-Fe_2O_3 was detected by XRD if the calcination was done at 500 °C. Among the three methods to add fructose and glucose, to add them into the final newly centrifuged precipitate brought more Fe_2O_3 in γ-Fe_2O_3 phase than α-Fe_2O_3 phase. It indicates that with more fructose and glucose in the precipitate, there is complete reduction of Fe^{3+} ion to Fe^{2+}.

For the promoted catalyst C and 26.3F26.3G-C, the Fe $2p_{3/2}$ BE is further decreased by the effect of electron donation from promoter K.[34]

3.4 *H_2-TPR of catalysts*

Figure 1b depicts the H_2-TPR files of precursor and catalyst prepared with the addition of fructose and glucose. Among the three precursors, P-26.3F26.3G-C is the easiest to be reduced. These results are consistent with the previous reports that the samples rich in γ-Fe_2O_3 phase were easier reduced than those rich in α-Fe_2O_3 phase.[16,19]

After the precursors were promoted with Cu and K, the reduction process happened at low temperature by the help of Cu.[20,23] Because neither Cu-containing particle nor K-containing particle is found by XRD in Figure S7 (Supplementary Information), both Cu and K are highly dispersive on the three catalysts. 26.3F26.3G-C has the largest surface area (Table S1, Supplementary Information). The dispersity of Cu is probably the highest on it than the others. As the result, the reduction peak of 26.3F26.3G-C is shifted to lower temperature related to the other two catalysts. The two characteristics, high dispersity and high reducibility related to γ-Fe_2O_3 phase, jointly bring forth more active site on 26.3F26.3G-C than 26.3F26.3G-A and 26.3F26.3G-B. This is responsible for the high CO_2 conversion on 26.3F26.3G-C (Table 1).

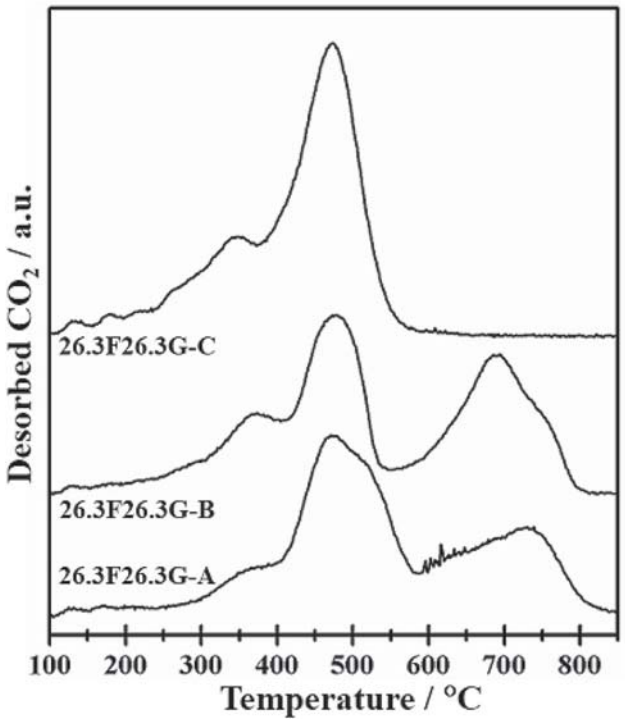

Figure 5. CO_2-TPD of catalysts prepared with fructose and glucose.

3.5 *CO_2-TPD*

Figure 5 contrasts the CO_2-TPD results of catalysts prepared with fructose and glucose. There are three peaks of CO_2 desorption from 26.3F26.3G-A (365 °C, 480 °C and 722 °C) and 26.3F26.3G-B (365 °C, 478 °C and 692 °C), but only two peaks from 26.3F26.3G-C (350 °C and 474 °C). The radius of K^{1+} (1.33 Å) is two times of Fe^{3+} (0.64 Å). So, promoter K mainly distributed on catalyst surface.[16,23] The sequence of surface area is 26.3F26.3G-B < 26.3F26.3G-A < 26.3F26.3G-C (Table S1). The dispersive degree of K probably increases in the above order. Promoter K can enhance CO_2 adsorption,[9,30,31,35–37] and CO_2 adsorbs on both the Fe and K.[34,35,37] The adsorption strength of CO_2 on aggregated K is higher than Fe,[11] which is reflected by the peaks around 700 °C for 26.3F26.3G-A and 26.3F26.3G-B. However, the strongly adsorbed CO_2 had difficulty to react with H_2 and resulted in a lower activity of 26.3F26.3G-A and 26.3F26.3G-B than 26.3F26.3G-C.[14]

4. Conclusions

Three methods are used to evaluate the influence of sucrose on FeAl catalysts. Sucrose is added into the mixed $Fe(NO_3)_3$ and $Al(NO_3)_3$ solution, or $(NH_4)_2CO_3$ solution, or the final newly centrifuged precipitate, respectively. Although the surface area of 50S-A is lower than 50S-B and 10S-C, it is the best one to hydrogenate CO_2 into C_{5+} hydrocarbons. The responsible factor is assigned to sucrose hydrolysis in acid solution. The evidence is found by dissolving sucrose in $Fe(NO_3)_3$ and $Al(NO_3)_3$ solution under 50 °C and 60 °C, which can enhance sucrose hydrolysis. γ-Fe_2O_3 phase is detected in the two samples.

With the inspiration from sucrose hydrolysis effect on catalytic performance, the hydrolysates, fructose and glucose are directly used to prepare catalysts. γ-Fe_2O_3 phase appears in all the samples in spite of the methods to add fructose and glucose. The purity of γ-Fe_2O_3 phase is the highest in the sample to add fructose and glucose into the final newly centrifuged precipitate, and the obtained catalyst (26.3F26.3G-C) is the most active one. It achieves CO_2 conversion of 30.3% and C_5 + selectivity of 52.2% under reaction conditions of H_2:CO_2 = 3:1, 6.0 L/(h·g-cat), 1.6 MPa and 235 °C.

Based on the observation of XPS, the formation of γ-Fe_2O_3 phase is explained as Fe^{3+} ion from $Fe(NO_3)_3$ is reduced into Fe^{2+} by fructose and glucose during the precipitation and drying, and the Fe^{2+} ion is re-oxidized into Fe^{3+} in the followed calcination. By the help of low temperature calcination at 350 °C, the formed iron oxide exists as metastable γ-Fe_2O_3, rather than the thermodynamically stable α-Fe_2O_3 phase.

Supplementary Information (SI)

Figures S1–S7 and Tables S1–S2 are available at www.ias.ac.in/chemsci.

Acknowledgements

This work was supported by the Zhejiang Provincial Natural Science Foundation of China [LY14B030003], and the National Ministry of Science and Technology of China [2014BAD02B05].

References

1. Najera M, Solunke R, Gardner T and Veser G 2011 Carbon capture and utilization via chemical looping dry reforming *Chem. Eng. Res. Des.* **89** 1533
2. Albrecht M, Rodemerck U, Schneider M, Bröring M, Baabe D and Kondratenko E V 2017 Unexpectedly efficient CO_2 hydrogenation to higher hydrocarbons over non-doped Fe_2O_3 *Appl. Catal. B* **204** 119
3. Mutschler R, Moioli E, Luo W, Gallandat N and Züttel A 2018 CO_2 hydrogenation reaction over pristine Fe, Co, Ni, Cu and Al_2O_3 supported Ru: Comparison and

determination of the activation energies *J. Catal.* **366** 139
4. Mattia D, Jones M D, O'Byrne J P, Griffiths O G, Owen R E, Sackville E, McManus M and Plucinski P 2015 Towards carbon-neutral CO_2 conversion to hydrocarbons *ChemSusChem* **8** 4064
5. Choi Y H, Jang Y J, Park H, Kim W Y, Lee Y H, Choi S H and Lee J S 2017 Carbon dioxide Fischer–Tropsch synthesis: A new path to carbon-neutral fuels *Appl. Catal. B* **202** 605
6. Díez-Ramírez J, Sánchez P, Kyriakou V, Zafeiratos S, Marnellos G E, Konsolakis M and Dorado F 2017 Effect of support nature on the cobalt-catalyzed CO_2 hydrogenation *J. CO_2 Util.* **21** 562
7. Yang H, Zhang C, Gao P, Wang H, Li X, Zhong L, Wei W and Sun Y 2017 A review of the catalytic hydrogenation of carbon dioxide into value-added hydrocarbons *Catal. Sci. Technol.* **7** 4580
8. Liu B, Geng S, Zheng J, Jia X, Jiang F and Liu X 2018 Unravelling the new roles of Na and Mn promoter in CO_2 hydrogenation over Fe_3O_4-based catalysts for enhanced selectivity to light α-olefins *ChemCatChem* **10** 4718
9. Riedel T, Claeys M, Schulz H, Schaub G, Nam S-S, Jun K-W, Choi M-J, Kishan G and Lee K-W 1999 Comparative study of Fischer-Tropsch synthesis with H_2/CO and H_2/CO_2 syngas using Fe- and Co-based catalysts *Appl. Catal. A* **186** 201
10. Zhang Y, Jacobs G, Sparks D E, Dry M E and Davis B H 2002 CO and CO_2 hydrogenation study on supported cobalt Fischer-Tropsch synthesis catalysts *Catal. Today* **71** 411
11. Satthawong R, Koizumi N, Song C and Prasassarakich P 2015 Light olefin synthesis from CO_2 hydrogenation over K-promoted Fe-Co bimetallic catalysts *Catal. Today* **251** 34
12. Ning W, Koizumi N and Yamada M 2009 Researching Fe catalyst suitable for CO_2-containing syngas for Fischer–Tropsch synthesis *Energy Fuels* **23** 4696
13. Dorner R W, Hardy D R, Williams F W and Willauer H D 2010 K and Mn doped iron-based CO_2 hydrogenation catalysts: Detection of $KAlH_4$ as part of the catalyst's active phase *Appl. Catal. A* **373** 112
14. Ning W, Li B, Wang B, Yang X and Jin Y 2019 Enhanced production of C_{5+} hydrocarbons from CO_2 hydrogenation by the synergistic effects of Pd and K on γ-Fe_2O_3 catalyst *Catal. Lett.* **149** 431
15. Wei J, Ge Q, Yao R, Wen Z, Fang C, Guo L, Xu H and Sun J 2017 Directly converting CO_2 into a gasoline fuel *Nat. Commun.* **8** 15174
16. Ning W, Wang T, Chen H, Yang X and Jin Y 2017 The effect of Fe_2O_3 crystal phases on CO_2 hydrogenation *PLoS ONE.* **12** e0182955
17. Liu J, Zhang A, Jiang X, Liu M, Zhu J, Song C and Guo X 2018 Direct transformation of carbon dioxide to value-added hydrocarbons by physical mixtures of Fe_5C_2 and K-modified Al_2O_3 *Ind. Eng. Chem. Res.* **57** 9120
18. Drab D M, Willauer H D, Olsen M T, Ananth R, Mushrush G W, Baldwin J W, Hardy D R and Williams F W 2013 Hydrocarbon synthesis from carbon dioxide and hydrogen: A two-step process *Energy Fuels* **27** 6348
19. Chen H-X, Ning W-S, Chen C-H and Zhang T 2015 Influence of Fe_2O_3 crystal phase on the performance of Fe-based catalysts for CO_2 hydrogenation *J. Fuel Chem. Technol.* **43** 1387
20. Bukur D B, Mukesh D and Patel S A 1990 Promoter effects on precipitated iron catalysts for Fischer–Tropsch synthesis *Ind. Eng. Chem. Res.* **29** 194
21. Ning W, Yang X and Yamada M 2012 Influence of palladium on the hydrocarbon distribution of Fischer-Tropsch reaction over precipitated iron catalyst *Curr. Catal.* **1** 88
22. Herranz T, Rojas S, Pérez-Alonso F J, Ojeda M, Terreros P and Fierro J L G 2006 Carbon oxide hydrogenation over silica-supported iron-based catalysts Influence of the preparation route *Appl. Catal. A* **308** 19
23. Ning W, Yang S, Chen H and Yamada M 2013 Influences of K and Cu on coprecipitated FeZn catalysts for Fischer–Tropsch reaction *Catal. Commun.* **39** 74
24. Echeverria E 1990 Developmental transition from enzymatic to acid hydrolysis of sucrose in acid limes (*Citrus aurantifolia*) *Plant Physiol.* **92** 168
25. Das R N 2001 Nanocrystalline ceramics from sucrose process *Mater. Lett.* **47** 344
26. Wu Y, Bandyopadhyay A and Bose S 2004 Processing of alumina and zirconia nano-powders and compacts *Mater. Sci. Eng. A* **380** 349
27. Girardon J-S, Quinet E, Griboval-Constant A, Chernavskii P A, Gengembre L and Khodakov A Y 2007 Cobalt dispersion, reducibility, and surface sites in promoted silica-supported Fischer–Tropsch catalysts *J. Catal.* **248** 143
28. Ribeiro A T S, Bezerra V V L, Bartolomeu R A C, Abreu C A M, Filho N M L, Silva A O S, Maranhão L C A, Merino D, Sanz O, Montes M, Machado G and Almeid L C 2018 Influence of sucrose addition and acid treatment of silica-supported Co-Ru catalysts for Fischer–Tropsch synthesis *Fuel* **231** 157
29. Ha K-S, Jung G-I, Woo M-H, Jun K-W and Bae J W 2013 Effects of phosphorus and saccharide on size, shape, and reducibility of Fischer–Tropsch catalysts for slurry phase and fixed-bed reactions *Appl. Catal. A* **453** 358
30. Boreriboon N, Jiang X, Song C and Prasassarakich P 2018 Fe-based bimetallic catalysts supported on TiO_2 for selective CO_2 hydrogenation to hydrocarbons *J. CO_2 Util.* **25** 330
31. Shi Z, Yang H, Gao P, Chen X, Liu H, Zhong L, Wang H, Wei W and Sun Y 2018 Effect of alkali metals on the performance of $CoCu/TiO_2$ catalysts for CO_2 hydrogenation to long-chain hydrocarbons *Chin. J. Catal.* **39** 1294
32. Grosvenor A P, Kobe B A, Biesinger M C and McIntyre N S 2004 Investigation of multiplet splitting of Fe 2p XPS spectra and bonding in iron compounds *Surf. Interface Anal.* **36** 1564
33. Nesbitt H W and Muir I J 1994 X-ray photoelectron spectroscopic study of a pristine pyrite surface reacted with water vapour and air *Geochim. Comochim. Acta* **58** 4667

34. Dry M E, Shingles T, Boshoff L J and Oosthuizen G J 1969 Heats of chemisorption on promoted iron surfaces and the role of alkali in Fischer–Tropsch synthesis *J. Catal.* **15** 190
35. Choi P H, Jun K-W, Lee S-J, Choi M-J and Lee K-W 1996 Hydrogenation of carbon dioxide over alumina supported Fe-K catalysts *Catal. Lett.* **40** 115
36. Xu L, Wang Q, Liang D, Wang X, Lin L, Cui W and Xu Y 1998 The promotions of MnO and K_2O to Fe/silicalite-2 catalyst for the production of light alkenes from CO_2 hydrogenation *Appl. Catal. A* **173** 19
37. Yan S-R, Jun K-W, Hong J-S, Choi M-J and Lee K-W 2000 Promotion effect of Fe–Cu catalyst for the hydrogenation of CO_2 and application to slurry reactor *Appl. Catal. A* **194–195** 63